

# Antiferromagnetism and Superconductivity in a model of Quasi 1D Organic Conductors

S. Moukouri

*Department of Physics and Michigan Center for Theoretical Physics  
University of Michigan, 2477 Randall Laboratory, Ann Arbor MI 48109*

I apply a two-step renormalization group method to the study of the competition between antiferromagnetism (AFM) and superconductivity in an anisotropic 2D Hubbard model. I show that this simple model captures the essentials of the ground-state phases of the quasi 1D organic conductors. As found experimentally, the ground-state phase diagram is mostly AFM. The AFM is localized in the strong-coupling limit where the electrons are confined in the chains. It is an SDW in the weak-coupling limit where interchain hopping is present. There is a tiny region in the weak-coupling regime where transverse two-particle hopping is dominant over magnetism.

*Introduction.* The intriguing discovery of superconductivity (SC) lying next to antiferromagnetism (AFM) in the phase diagram of the charge transfer Bechgaard salts (see Fig.1) remains one of the greatest issues of condensed matter physics [14]. The proximity of AFM and SC turned out to be a generic feature not only of the Bechgaard salt series  $(TMTSF)_2X$ , but also of the Fabre salts  $(TMTTF)_2X$  and layered 2D organic and cuprate superconductors. In the quasi 1D organic materials, AFM occupies a large region of the phase diagram and is believed to be central to the emergence of SC. It is believed that the understanding of AFM is a prerequisite to that of SC.

The nature of pairing in these compounds is still unclear. Recent experiments have yielded conflicting results. A NMR Knight shift experiment by Lee et al. [12] found that the symmetry of the Cooper pairs is triplet in  $(TMTSF)_2(PF)_6$ . No shift was found in the magnetic susceptibility at the transition for measurement made under a magnetic field of about 1.4 *Tesla*. A subsequent Knight shift experiment performed at lower fields reveals a decrease in the spin susceptibility. This result is consistent with singlet pairing.[16] The authors of this later experiment suggested a possible singlet-triplet pairing crossover as function of the magnetic field as a resolution of these conflicting results.

In the face of these experimental uncertainties, a theoretical input onto the behavior of simple models of these compounds is of crucial importance. A theoretical analysis of AFM in the quasi 1D organic materials was proposed by Bourbonnais, Caron, and coworkers [1]. This description was essentially based on a perturbative renormalization group (RG) applied on the g-ology model. They found that the AFM phase has two regions. On the left side of the AFM phase, the 1D chains are Mott insulators, the charge gap  $\Delta_\rho$  induced by coulomb interactions is such that  $\Delta_\rho \gg t_\perp$ , where  $t_\perp$  is the transverse hopping parameter. Hence, the single particle transverse hopping is irrelevant. In this region, the electrons are necessarily confined in the chains.  $t_\perp$  can nevertheless generate an interchain exchange  $J_\perp$  by virtual interchain

hopping. Using the RG method [2], it can be shown that this process leads to a transverse effective Hamiltonian  $H_\perp = \int dx \sum_i J_\perp S(x)_i S(x)_{i+1}$ , with  $J_\perp \approx t_\perp^2 / \Delta_\rho$ . In this region, the electrons are necessarily confined in the chains due to the irrelevance of  $t_\perp$ . As pressure increases, the electrons progressively delocalize in the transverse direction. In the right region of the AFM phase, the magnetism is itinerant and arises from the nesting of the Fermi surface  $\epsilon_{r,l}(k) = -\epsilon_{l,r}(k+Q)$ , where the indices  $(r,l)$  stand for the right and the left parts of the Fermi surface respectively, and  $Q = (2k_F, \pi)$  is the nesting vector. The nesting leads to the divergence of the susceptibility  $\chi(Q, \omega = 0) \propto \frac{1}{L^2} \sum_k \frac{f(\epsilon_r(k)) - f(\epsilon_l(k+Q))}{\epsilon_r(k) - \epsilon_l(k+Q)}$ . However, this description presents a difficulty. At a temperature above the SDW phase, the system is not a Fermi liquid, it is rather a Luttinger liquid. There are no quasi particles and the FL description does not apply. A perturbative RG applied for coupled LLs can only yield the most divergent susceptibility, but it cannot reach the ordered phase. Further increasing pressure destroys the magnetic order and leads to superconductivity as illustrated on the right part of the phase diagram. A recent RG analysis has suggested that superconductivity can emerge from the frustration induced by hopping between next-nearest neighbors chains [25]. Pairing emerges through short-range AFM analogous to the Kohn-Luttinger effect induced by Friedel oscillations[11].

*Model and Methods.* The Hubbard model is also often used for the organic conductors. It differs from the g-ology model in that it includes non-linear dispersion and the scattering processes are not restricted to a narrow region around the Fermi points. While it enjoys an exact solution and can be studied with the density-matrix renormalization group (DMRG) or the Monte Carlo methods in 1D, it remains a difficult challenge, even numerically, when  $t_\perp$  is turned on. In this letter, I will show that the essential aspects of the ground-state phase diagram can be obtained from the single-band extended Hubbard model using the two-step DMRG method [6, 7], to which I supplement with a Wilson RG analysis of the low energy spectrum. I will consider the following model

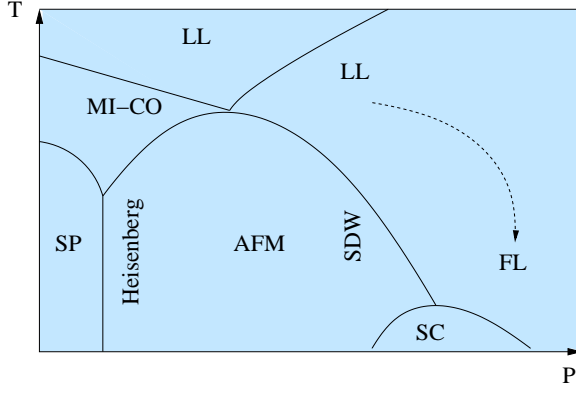


FIG. 1: Sketch of generic phase diagram of the quasi 1D organic conductors: LL (Luttinger Liquid), FL (Fermi Liquid), MI (Mott Insulator), CO (Charge Ordering), SP (Spin-Peierls), AFM (Antiferromagnet), SC (Superconductor).

at quarter filling, the nominal density of organic conductors, which has standard notations:

$$\begin{aligned}
 H = & -t_{\parallel} \sum_{i,l,\sigma} (c_{i,l,\sigma}^{\dagger} c_{i+1,l,\sigma} + h.c.) + U \sum_{i,l} n_{i,l,\uparrow} n_{i,l,\downarrow} \\
 & + V \sum_{i,l,\sigma} n_{i,l,\sigma} n_{i+1,l,\sigma} - \mu \sum_{i,l,\sigma} n_{i,l,\sigma} \\
 & - t_{\perp} \sum_{i,l,\sigma} (c_{i,l,\sigma}^{\dagger} c_{i,l+1,\sigma} + h.c.) + V_{\perp} \sum_{i,l,\sigma} n_{i,l,\sigma} n_{i,l+1,\sigma}. \quad (1)
 \end{aligned}$$

The two-step RG method starts by using DMRG to compute the low energy eigenvalues and eigenvectors of a single chain of length  $L$ . Then Hamiltonian  $H$  is projected onto the tensor product of the eigenvectors of the disconnected chains. This leads to the effective one-dimensional Hamiltonian

$$\begin{aligned}
 \tilde{H} \approx & \sum_l H_{0,l} - t_{\perp} \sum_{l,\sigma} (\tilde{c}_{l,\sigma}^{\dagger} \tilde{c}_{l+1,\sigma} + h.c.) \\
 & + V_{\perp} \sum_{i,l,\sigma} \tilde{n}_{i,l,\sigma} \tilde{n}_{i,l+1,\sigma}, \quad (2)
 \end{aligned}$$

where  $H_{0,l}$  is diagonal, its elements are the eigenvalues of the single chain, the operators  $\tilde{c}_{l,\sigma}$  are composite matrices containing the renormalized  $c_{i,l,\sigma}$  for  $i = 1, L$ . Since  $\tilde{H}$  is 1D, it may be studied using DMRG again.

Additional insight in the behavior of  $H$  may be gained by using the Wilson RG instead of DMRG in the second step. The advantage of the Wilson RG lies in the fact that the low energy spectrum can be obtained. However the Wilson method, directly applied to  $\tilde{H}$ , is not accurate because all the terms in the transverse direction are of the same order. I use the same trick used by Wilson for the Kondo problem [26].  $\tilde{H}$  is defined as the limit of  $\tilde{H}_{\Lambda}$  when  $\Lambda \rightarrow 1$ .  $\tilde{H}_{\Lambda}$  is given by

$$\tilde{H}_{\Lambda} = \sum_l \frac{H_{l,l+1}}{\Lambda^{(l-1)/2}}, \quad (3)$$

where

$$\begin{aligned}
 H_{l,l+1} = & H_{0,l} + H_{0,l+1} - t_{\perp} \sum_{\sigma} (\tilde{c}_{l,\sigma}^{\dagger} \tilde{c}_{l+1,\sigma} + h.c.) \\
 & + V_{\perp} \sum_{i,l,\sigma} \tilde{n}_{i,l,\sigma} \tilde{n}_{i,l+1,\sigma}. \quad (4)
 \end{aligned}$$

It is to be noted that this is not the usual Wilson's momentum space discretization. The justification of this scheme rests on the fact that the essential physics remains unchanged. When  $\Lambda > 1$ , the terms corresponding to  $l > 1$  act as a perturbation on the term with  $l = 1$ . For  $\Lambda$  not too large, I expect  $\tilde{H}_{\Lambda}$  to essentially have the same behavior as  $\tilde{H}$ . But if  $\lambda \gg 1$ ,  $t_{\perp}/\Lambda$  will be too small with respect to the finite size energy separation and the chains will be disconnected. It is to be remarked that this approach may also be useful if it is embedded as a cluster solver in a chain-dynamical mean-field approach [4].

*Results.* The pressure variation will be mimicked by varying the Coulomb parameters  $U$  and  $V$ , while I keep  $t_{\parallel}$ ,  $t_{\perp}$  and  $V_{\perp}$  constant in most simulations. In the regime of strong  $U$  and  $V$ , the isolated chains are Mott insulators, there is a large charge gap  $\Delta_{\rho}$  while the spin degrees of freedom are gapless. At  $V \lesssim 2$  for any value of  $U$ , there is a insulator-metal transition [23]. The transverse correlation functions yield information on which type of order will dominate. Since the parallel correlations have a power law decay in absence of a gap, the most dominant transverse correlation in a given channel will automatically lead to long-range order in that channel, even if it is not dominant in 1D. Before performing the analysis of the transverse correlations, it is somewhat instructive to look at the low energy spectrum provided by the Wilson method. This will allow to make a qualitative comparison with the evolution under pressure with the prediction of the perturbative RG.

The low energy-excitation spectrum of  $\tilde{H}$  was obtained from the Wilson RG for  $\Lambda \approx 1.2$  for a lattice size  $16 \times 6$ , keeping 100 states block. The lowest 1000 excited states are shown in Fig.2. They are drastically different as pressure is varied. In the confined regime for  $U = 6$   $V = 2$  Fig.2, all the lowest states have the charge  $\lambda_n = 0$ . This is consistent with the fact that since  $t_{\perp} \ll \Delta_{\rho}$ , the low energy behavior of  $\tilde{H}$  is roughly identical to that of an Heisenberg model, only spin excitations are allowed. This is typically the regime of Fabre salts at ambient pressure where a large charge gap is observed in optical conductivity measurements [21]. By contrast, in the SDW regime for  $U = 4$   $V = 0.85$ , spins excitation are still the lowest

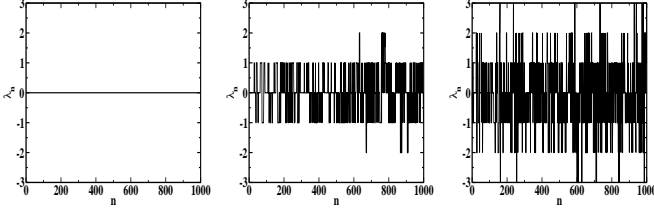


FIG. 2: Charge  $\lambda_n$  of lowest 1000 excitations after 6 RG iterations, the lattice size is  $16 \times 6$ , for  $\Lambda = 1.2$ : in the localized AFM  $U = 6$ ,  $V = 2$  (left), the SDW  $U = 4$ ,  $V = 0.85$  (center), and superconductor  $U = 2$ ,  $V = 0$  (right)

but excitations with  $\lambda = \pm 1$  now appear above them. Excitations with  $\lambda = \pm 2$  are also observed at higher energy. It is to be noted that because of numerical errors, excitations with  $\lambda_n = 1$  and  $\lambda_n = -1$  which should normally have the same energy are shifted. In the regime with important superconductive correlations  $U = 2$ ,  $V = 0$ , excitations with  $\lambda = \pm 2$  now appear closer to the ground state. This is consistent with the increase of superconductive correlations as we found below.

I now analyse the evolution of the transverse correlations when  $U$  and  $V$  are varied using the two-step DMRG for the lattice size  $L_x \times L_y = 16 \times 17$ . I keep  $ms_1 = 256$  states during the first step and a maximum of  $ms_2 = 128$  states during the second step. For this value of  $ms_2$ ,  $\Delta E/t_\perp \approx 5$  which means that we are at the limit of the two-step method as discussed in Ref.8. Starting from the left of the AFM phase where  $U$  and  $V$  are expected to be strong, because of the presence of a large  $\Delta_\rho$ , the carriers are confined in the chains, even when  $t_\perp \ll \Delta_\rho$  is turned on. The carrier confinement was observed by Vescoli et. al in optical reflectivity measurements [22]. When the oscillating electric field was oriented in the transverse direction, no plasma mode was observed. This carrier confinement is seen in the behavior of the transverse Green's function  $G(y) = \langle c_{L/2, L/2+y} c_{L/2, L/2+y}^\dagger \rangle$ .  $G(y)$ , shown in Fig.3(a) for  $U = 6$  and  $V = 2$ , decays very fast.  $G(y) \approx 0$  for  $y > 3$ . This was expected given that  $t_\perp/\Delta_\rho \approx 0.1$ . But as predicted by the RG [1], although irrelevant,  $t_\perp$  can nevertheless generate the motion of transverse spin degrees of freedom and lead to magnetic order. This is seen in the transverse spin-spin correlation function  $C(y) = \frac{1}{3} \langle \mathbf{S}_{L/2, L/2+y} \mathbf{S}_{L/2, L/2+y} \rangle$  which is shown in Fig.3(b). I find that despite the irrelevance of  $t_\perp$ ,  $G(y)$  has its largest amplitude in the strong coupling limit. As expected I find that the transverse singlet (triplet) superconductive correlations  $SS(y) = 2 \langle \Delta_{L/2, L/2+y} \Delta_{L/2, L/2+y}^\dagger \rangle$  ( $ST(y) = 2 \langle \Theta_{L/2, L/2+y} \Theta_{L/2, L/2+y}^\dagger \rangle$ ), where  $\Delta_{i,l} = \frac{1}{\sqrt{2}}(c_{i,l\uparrow} c_{i+1,l\downarrow} - c_{i,l\downarrow} c_{i+1,l\uparrow})$  ( $\Theta_{i,l} = \frac{1}{\sqrt{2}}(c_{i,l\uparrow} c_{i+1,l\downarrow} + c_{i,l\downarrow} c_{i+1,l\uparrow})$ ), are negligible in this limit as seen in Fig.3(c)(d).

Moving toward the right of the phase diagram by in-

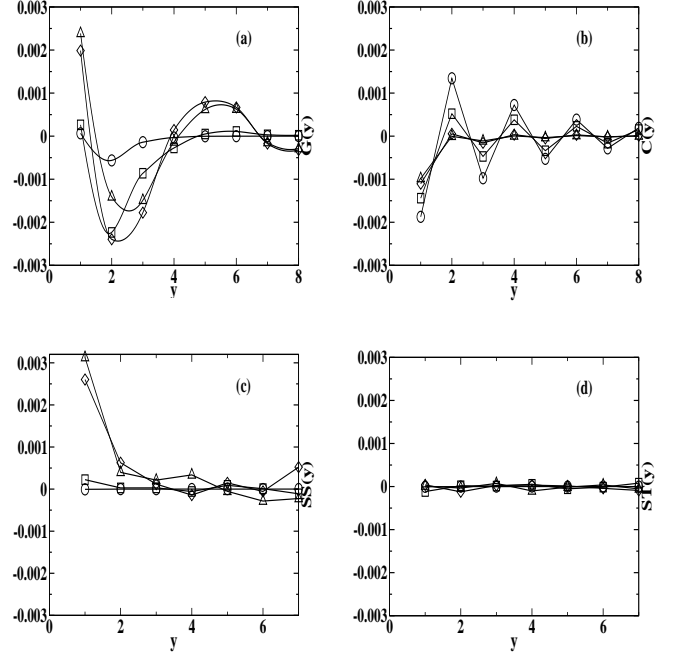


FIG. 3: Transverse interchain correlations as function of distance  $y$ : Green's function  $G(y)$  (a), spin-spin correlation  $C(y)$  (b), singlet superconductive  $SS(y)$  (c), triplet superconductive  $ST(y)$  (d) for  $U = 6$ ,  $V = 2$  (circles),  $U = 4$ ,  $V = 0.85$  (squares),  $U = 3$ ,  $V = 0$  (diamonds),  $U = 2$ ,  $V = 0$  (triangles).

creasing pressure or equivalently decreasing  $U$  and  $V$ , the carriers are expected to progressively deconfine. In this regime, the reflectivity measurements of Ref.22 reported the observation a transverse plasma mode. The carrier deconfinement is expected for  $t_\perp/\Delta_\rho \approx 0.5$ . For  $U = 4$  and  $V = 0.85$ , the numerical simulation yields  $t_\perp/\Delta_\rho \approx 0.3$ . In Fig.3(a),(b),(c),(d), it can be seen that for  $U = 4$  and  $V = 0.85$   $G(y)$  now has a non-zero amplitude,  $C(y)$  is still significant, while  $SS(y)$  and  $ST(y)$  are still very small. This suggests that the system is in the SDW phase. The perturbative RG, coming from high temperatures, shows that there is a 1D to 2D crossover at  $T_x \approx t_\perp/\pi$ . At  $T_x$  the 1D RG equations cease to be valid. FL arguments are used to describe the onset of the SDW order. The experimental observations are however that both the non-FL and FL characters seem to be present depending on the quantity measured [1]. A future application of the TS-DMRG at finite temperature could shed light on this interesting crossover regime.

If  $U$  and  $V$  are further reduced,  $C(y)$  now decays faster despite the fact that the amplitude of  $G(y)$  is larger.  $C(y)$  now vanishes for  $y > 3$  as seen in Fig.3(b) for  $U = 3$ ,  $U = 2$  and  $V = 0$  in both cases. This implies the absence of long-range magnetic order in this regime. At the same time,  $SS(y)$  sharply increases suggesting the onset of superconductivity in agreement with the phase dia-

gram. The values of  $SS(y)$  at long distances are however within our margin of error. The presence of  $V_{\perp}$  is crucial to the enhancement of pairing correlation. In the absence of  $V_{\perp}$ , if all other parameters are unchanged, the dominant correlations are AFM.  $ST(y)$  is still negligible thus suggesting the absence of triplet pairing in the extended Hubbard model. Experimental results on the symmetry of the pairs are still controversial. Knight shift experiments from different groups have predicted singlet [16] and triplet [12] pairings as discussed in the introduction. This study shows a tendency towards singlet-pairing only in the extended Hubbard model. Singlet pairing, though interchain, was also predicted by the perturbative RG. However, in the RG, the pairs could be formed by carriers lying on neighboring chains and AFM was suppressed by hopping to next-nearest neighbor chain. It was suggested in the RG study that the interchain pairing could be triplet in presence of strong enough next-nearest neighbor hopping and nearest neighbor Coulomb interaction both in the transverse direction. The present two-step results do not however settle this issue. Many small effects including longer range hopping and Coulomb interactions were not included in this simple model. Triplet superconductivity could emerge from these terms.

*Conclusion.* To summarize, I have shown that the single band extended Hubbard model displays the ground-state phases of the quasi 1D organic conductors: (i) localized magnetism in the strong-coupling regime, (ii) delocalized SDW magnetism in the intermediate coupling regime, and (iii) possible superconductivity of singlet type in the weak coupling regime. I have not discussed the spin-Peierls phase which rests at the extreme left of the phase diagram. In this regime, the electron-phonon coupling is dominant over the effective transverse exchange  $J_{\perp}$ , hence a pure 1D study of a spin model coupled to phonons such as that of Ref.[24], which shows a spin gap opening, captures this part of the phase diagram.

I am very grateful to C. Bourbonnais for very helpful exchanges. This work was supported by the NSF Grant No. DMR-0426775.

- 
- [1] C. Bourbonnais and L.G. Caron, Int. J. Mod. Phys. **B 5**, 1033 (1991).
  - [2] C. Bourbonnais and L.G. Caron, Europhys. Lett. **5**, 209 (1988).
  - [3] T. Giamarchi in "Quantum Physics in One Dimension", Clarendon Press Eds, P. 254-269 (2004).
  - [4] S. Biermann, A. Georges, A. Lichtenstein, and T. Giamarchi, Phys. Rev. Lett. **87**, 276405 (2001).
  - [5] S.R. White, D.J. Scalapino, R.L. Sugar, E.Y. Loh, J.E. Gubernatis, and R.T. Scalettar, Phys. Rev. **B 40**, 506 (1989).
  - [6] S. Moukouri, Phys. Rev. **B 70**, 014403 (2004).
  - [7] S. Moukouri, J. Stat. Mech. P02002 (2006).
  - [8] S. Moukouri, cond-mat/0704.1618 (2007).
  - [9] S.R. White, Phys. Rev. Lett. **69**, 2863 (1992). Phys. Rev. **B 48**, 10 345 (1993).
  - [10] S.R. White, Phys. Rev. **B 72**, 180403 (2005).
  - [11] V.J. Emery, Synthetic Metals, **13**, 21 (1986).
  - [12] I.J. Lee *et al.*, Phys. Rev. Lett. **88**, 017004 (2002).
  - [13] N. Dupuis, C. Bourbonnais and J.C. Nickel, cond-mat/0510544.
  - [14] D. Jerome and H.J. Schulz, Adv. Phys. **31**, 299 (1982).
  - [15] D. Jerome, Chem. Rev. **104**, 5565 (2004). D. Jerome and C.R. Pasquier, in Superconductors, edited by A.V. Narlikar (Springer Verlag, Berlin, 2005).
  - [16] Y. Shinagawa, *et al.*, cond-mat/0701566 (2007).
  - [17] Y. Tanaka and K. Kuroki, Phys. Rev. **B 70**, 060502 (2004).
  - [18] Mahito Kohmoto and Masatoshi Sato, cond-mat/0001331 (2000).
  - [19] I.J. Lee, M.J. Naughton, P.M. Chaikin, Physica **B 294-295**, 413 (2001).
  - [20] S. R. White, Ian Affleck, and D. J. Scalapino, Phys. Rev. **B 65**, 165122 (2002).
  - [21] A. Schwartz *et al.*, Phys. Rev. **B 58**, 1261 (1998).
  - [22] V. Vescoli *et al.*, Science **281**, 1181 (1998).
  - [23] F. Mila and X. Zotos, Europhys. Lett. **24**, 133 (1993).
  - [24] L. G. Caron and S. Moukouri, Phys. Rev. Lett. **76**, 4050 (1996).
  - [25] J.C. Nickel *et al.* Phys. Rev. Lett. **95** 247001 (2005).
  - [26] K.G. Wilson Rev. Mod. Phys. **47**, 773 (1975).